Communication

Micellar Cobaltporphyrin Nanorods in Alcohols

Makoto Yuasa, Kenichi Oyaizu, Aritomo Yamaguchi, and Michi Kuwakado

J. Am. Chem. Soc., **2004**, 126 (36), 11128-11129• DOI: 10.1021/ja0486216 • Publication Date (Web): 17 August 2004

J|A|C|S
COMMUNICATIONS

Published on Web 08/17/2004

Micellar Cobaltporphyrin Nanorods in Alcohols

Makoto Yuasa,*,†,‡ Kenichi Oyaizu,‡ Aritomo Yamaguchi,† and Michi Kuwakado†

Department of Pure and Applied Chemistry, Faculty of Science and Technology, Tokyo University of Science, Noda 278-8510, Japan, and Institute of Colloid and Interface Science, Tokyo University of Science, Tokyo 162-8601, Japan

Received March 10, 2004; E-mail: yuasa@rs.noda.tus.ac.jp

Here we communicate that cobalt(II) *meso*-tetrakis(4-hexadecylamidophenyl)porphyrin (CoTAPP) self-assembles in ethanol/1-propanol 2/1 (v/v) to form a rodlike micelle with nanoscale dimensions. Static light-scattering (SLS) and spectroscopic experiments reveal that the nanorod is a face-to-face aggregate having a hydrophobic corona around a polar core and is thus characterized as a reverse micelle. The alcoholic micellar solution has no precedent, to the best of our knowledge.

Porphyrins are major building blocks for self-assembled supramolecular systems based on $\pi-\pi$ stacking interactions.[1−3] In water, a variety of porphyrin amphiphiles are known to self-organize into micellar fibers,[4−8] while in organic solutions, examples are not as frequent as those involving zinc(II) porphyrins.[9−12] By analogy to reverse micelles, which provide a stable dispersion of water in nonpolar solvents,[13] we have anticipated that porphyrins bearing polar amido groups with which peripheral long alkyl chains are linked would self-organize even in nonaqueous media, leading to long-lived micelles stabilized through hydrogen bonding and hydrophobic interactions. We present here the properties of a reverse micelle made up of CoTAPP that exhibits a remarkable nanorod behavior.

The length of micellar neutral nanorods is an exponential function of the end-cap energy/thermal energy ratio[9] and is usually large even at low concentrations. Indeed, no critical micellar concentration (cmc) could be determined for the equilibrated solution of CoTAPP in ethanol/1-propanol 2/1 (v/v). However, the rate of spontaneous aggregation was very slow and required ultrasonic irradiation. The refractive index of the solution was used as a measure of aggregation, which slowly and irreversibly increased with the ultrasonic irradiation for several hours. The differential refractive index for the equilibrated solution increased linearly with the concentration of CoTAPP. Significant broadening of the Soret band (Figure S1, Supporting Information) was also suggestive of the aggregation. Attempts to delineate the micelles by freeze-fracture electron microscopy met with failure. Reasoning that replication of frozen alcohols might be disfavored because of the depression of the freezing point, we turned to SLS and dynamic light-scattering (DLS) studies. In SLS, the reduced light-scattering intensity $R(\theta)$ was interpreted using the equation $Kc/R(\theta) = [1 + \{16\pi^2R_G^2\sin^2(\theta/2)\}/(3\lambda^2)]/M_w + 2A_2c$, where K was the optical constant,[14] c was the concentration of CoTAPP, R_G was the radius of gyration, λ was the wavelength in a vacuum, M_w was the weight-averaged molecular weight, and A_2 was the second virial coefficient.[15] Extrapolating $Kc/R(\theta)$ to zero concentration (Figure 1A) yielded $M_w = 1.40 \times 10^6$ and $R_G = 59.3$ nm, while an extrapolation to zero angle (Figure 1B) yielded $M_w = 1.38 \times 10^6$ and $A_2 = 1.44 \times 10^{-1}$ cm^3 mol g^{-2}. The molecular weight corresponded to an aggregation number of $n \approx 800$.

† Department of Pure and Applied Chemistry.
‡ Institute of Colloid and Interface Science.

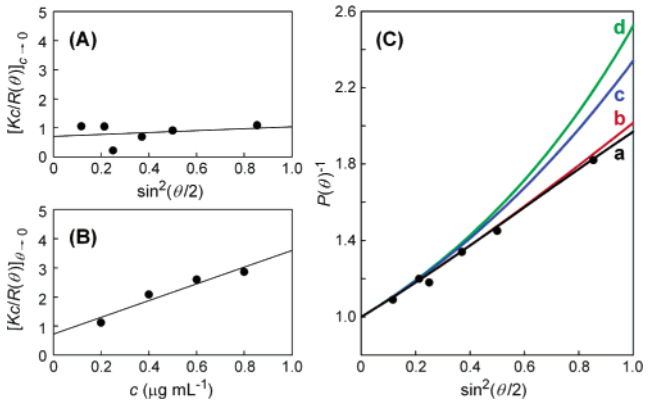

Figure 1. (A) Scattering data for an equilibrated solution of CoTAPP in ethanol/1-propanol 2/1 (v/v) at 298 K extrapolated to zero concentration versus $\sin^2(\theta/2)$. (B) Scattering data extrapolated to zero angle as a function of c. (C) The reciprocal of the scattering factor $P(\theta)$ as a function of $\sin^2(\theta/2)$ calculated from $P(\theta)^{-1} = M_w[Kc/R(\theta)]_{c\to 0}$. Curves correspond to the theoretical scattering factor calculated for (a) rods $(1 - x^2/9 + 2x^4/225$, where $x = ql/2$ and l (rod length) $= 3.46R_G)$, (b) spheres $(1 - x^2/5 + 3x^4/25$, where $x = qr$ and r (sphere radius) $= 1.29R_G)$, (c) random coils $(1 - x^2/3 + x^4/12$, where $x = q\langle r^2\rangle^{1/2}/6$ and $\langle r^2\rangle^{1/2}$ (mean end-to-end distance) $= 2.45R_G)$, and disks $(1 - x^2/6 + x^4/72 - x^6/1440 + x^8/43\,200$, where $x = qr$ and r (disk radius) $= 1.41R_G)$ using $q = (4\pi n_0/\lambda)\sin(\theta/2)$ and $\lambda = 633$ nm.

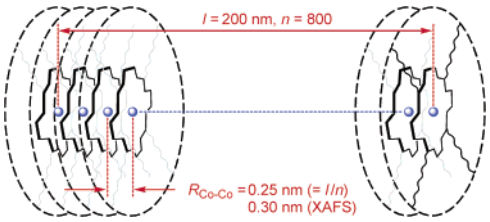

Figure 2. Schematic structure and dimensions of the face-to-face CoTAPP aggregate in the alcoholic micellar solution.

The SLS data were consistent with DLS results, which gave a hydrodynamic diameter of $\phi_{av} = 120$ nm (Figure S2, Supporting Information). The positive A_2 value was indicative of the repulsive interaction between the micelles, which would depress further flocculation of the micelles. The scattering factor $P(\theta)$ allowed prediction of the shape of the isolated micelle. Figure 1C shows plots of the scattering data superimposed on theoretically derived curves for various shapes of particles, which indicated that the micelle was a rod in shape with a length $l = 205$ nm.

Figure 2 illustrates the proposed structure and the dimension of the aggregate. Added support for the face-to-face orientation of CoTAPP was furnished by extended X-ray absorption fine structure (EXAFS) spectroscopy. The Fourier-transformed EXAFS function (Figure S3, Supporting Information) yielded an atomic distance $R_{Co-Co} = 0.30$ nm and a first-shell cobalt−cobalt coordination number of 0.9 ± 0.86, which was suggestive of the infinite chain

10.1021/ja0486216 CCC: $27.50

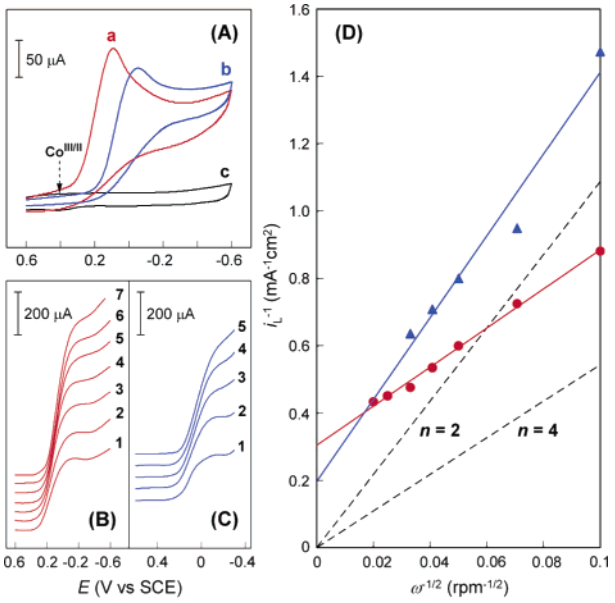

Figure 3. (A) Cyclic voltammogram for the reduction of O_2 at edge-plane pyrolytic graphite electrodes (0.28 cm^2) coated with 1.6×10^{-10} mol cm^{-2} of CoTAPP. The supporting electrolyte, 1 M $HClO_4$, was saturated with O_2 (curves a and b) or argon (curve c). CoTAPP was deposited on the electrode surface by transferring a pristine solution of CoTAPP in ethanol/1-propanol 2/1 (v/v) to record curve b or a micellar solution of CoTAPP prepared by ultrasonic irradiation of the pristine solution for 6 h to record curves a and c. The electrodes were covered with 8 μL of 0.5 wt % Nafion in 2-propanol and air-dried. Scan rate = 0.1 V s^{-1}. (B) Reduction of O_2 with the electrode used to record curve a operated as a rotating disk electrode under O_2. Electrode rotation rates were 100, 200, 400, 600, 900, 1600, and 2500 rpm for curves 1−7, respectively. (C) Reduction of O_2 with the electrode used to record curve b in A. Electrode rotation rates were 100, 200, 400, 600, and 900 rpm for curves 1−5, respectively. (D) Koutecky−Levich plots of (plateau current)$^{-1}$ versus (rotation rate)$^{-1/2}$ for the curves in B (●) and C (▲). The broken lines were calculated for the diffusion-convection-controlled reduction of O_2 by two (n = 2) or four (n = 4) electrons.

of the stacked CoTAPP molecules. The dimension was in good agreement with the cobalt−cobalt distance of l/n = 0.25 nm based on the SLS experiments.

Another curious feature is the electrocatalysis of O_2 reduction by the CoTAPP aggregate adsorbed at the surface of a graphite electrode immersed in an aqueous electrolyte solution. To determine the effect of the cofacial orientation on the catalytic activity, one can take advantage of the insolubility of CoTAPP in H_2O and the very slow rate of aggregation in alcohols. Thus, a pristine alcoholic solution of CoTAPP is presumed to contain the monomeric complex alone, while the rodlike aggregate formed after ultrasonic irradiation should survive during the electrode preparation and electrochemical measurements. Indeed, when these solutions were used as mother liquors to prepare the modified electrode by dip-coating, a quite different electrochemical response was obtained. In Figure 3A, curves a and b represent cyclic voltammograms for the reduction of O_2 at the modified electrode coated with the aggregate and the monomeric complex, respectively. A positive shift in the O_2 reduction potential was accomplished by the aggregation of CoTAPP, while the Co(III/II) couple was almost unaffected by the aggregation and appeared at an even more positive potential (0.41 V) in the absence of O_2 (curve c).

Figures 3B and 3C show current−potential curves for the reduction of O_2 at a rotating disk electrode coated with the aggregate and the monomeric complex, respectively. While the reduction occurred in a single step for both electrodes, the plateau current at the slowest rotation rate (curve 1) was nearly doubled by the conversion of the coating from the monomeric complex to the aggregate. Koutecky−Levich plots (Figure 3D) revealed that the aggregate reduced O_2 mainly with four electrons (n_{app} = 3.7), while a two-electron reduction was predominant for the monomeric complex (n_{app} = 2.0). Such a difference in the reactivity stems from the presence of two parallel reactions,[16] one involving the binding of O_2 to two proximate cobalt centers in the aggregate and giving rise to the four-electron reduction of O_2 to H_2O and the other involving a single cobalt center and yielding the two-electron reduction of O_2 to H_2O_2. Covalently linked cofacial metalloporphyrins[17−20] have been the typical platform for exploring such a cooperative effect of metal centers in promoting the four-electron reduction of O_2. The short cobalt−cobalt distance in the CoTAPP aggregate precludes O_2 binding, suggesting that O_2 is reduced at fracture or defect points with a larger cobalt−cobalt separation.

In conclusion, the alcoholic solution of CoTAPP provided simple systems developing the rodlike morphology that served as a template for the cofacial orientation of porphyrins at the electrode surface, allowing for both ends of O_2 molecules to interact with the cobalt centers in the transition state. Tuning the cobalt−cobalt distance within the micelle and the microscopic analysis of the nanorod are the topics of our continuous research.

Supporting Information Available: Details of the preparation of CoTAPP, the absorption spectrum, the DLS histogram, and the k^3-weighted EXAFS function of the aggregate (PDF). This material is available free of charge via the Internet at http://pubs.acs.org.

References

(1) Uno, H.; Masumoto, A.; Ono, N. *J. Am. Chem. Soc.* **2003**, *6*, 12082−12083.
(2) Shirakawa, M.; Kawano, S.; Fujita, N.; Sada, K.; Shinkai, S. *J. Org. Chem.* **2003**, *68*, 5037−5044.
(3) Kano, K.; Fukuda, K.; Wakami, H.; Nishiyabu, R.; Pasternack, R. F. *J. Am. Chem. Soc.* **2000**, *122*, 7494−7502.
(4) Komatsu, T.; Yanagimoto, T.; Furubayashi, Y.; Wu, J.; Tsuchida, E. *Langmuir* **1999**, *15*, 4427−4433.
(5) Komatsu, T.; Yamada, K.; Tsuchida, E.; Siggel, U.; Böttcher, C.; Fuhrhop, J.-H. *Langmuir* **1996**, *12*, 6242−6249.
(6) Fuhrhop, J.-H.; Bindig, U.; Siggel, U. *J. Am. Chem. Soc.* **1993**, *115*, 11036−11037.
(7) Fuhrhop, J.-H.; Bindig, U.; Siggel, U. *J. Chem. Soc., Chem. Commun.* **1994**, 1583−1584.
(8) Fuhrhop, J.-H.; Demoulin, C.; Böttcher, C.; Köning, J.; Siggel, U. *J. Am. Chem. Soc.* **1992**, *114*, 4159−4165.
(9) Terech, P.; Scherer, C.; Lindner, P.; Ramasseul, R. *Langmuir* **2003**, *19*, 10648−10653.
(10) Smith, K. M.; Kehres, L. A.; Fajer, J. *J. Am. Chem. Soc.* **1983**, *105*, 1387−1389.
(11) Jesorka, A.; Balaban, T. S.; Holzwarth, A. R.; Schaffner, K. *Angew. Chem., Int. Ed. Engl.* **1996**, *35*, 2861−2863.
(12) Tamiaki, H.; Kubota, T.; Tanikaga, R. *Chem. Lett.* **1996**, 639−640.
(13) Aoudia, M.; Rodgers, M. A. J. *J. Phys. Chem. B* **2003**, *107*, 6194−6207.
(14) Optical constant K was given by $4\pi^2 n_0^2 (dn/dc)^2 \lambda^{-4} N_A^{-1}$, with n_0 and n being the refractive index of the pure solvent and the solution, respectively, dn/dc the refractive index increment, and N_A Avogadro's constant.
(15) *Light Scattering from Polymer Solutions*; Huglin, M. B., Ed.; Academic Press: New York, 1972.
(16) Shi, C.; Steiger, B.; Yuasa, M.; Anson, F. C. *Inorg. Chem.* **1997**, *36*, 4294−4295.
(17) Chang, C. J.; Deng, Y.; Shi, C.; Chang, C. K.; Anson, F. C.; Nocera, D. G. *Chem. Commun.* **2000**, 1355−1356.
(18) Guilard, R.; Brandès, S.; Tardieux, C.; Tabard, A.; L'Her, M.; Miry, C.; Gouerec, P.; Knop, Y.; Collman, J. P. *J. Am. Chem. Soc.* **1995**, *117*, 11721−11729.
(19) Ni, C.-L.; Abdalmuhdi, I.; Chang, C. K.; Anson, F. C. *J. Phys. Chem.* **1987**, *91*, 1158−1166.
(20) Durand, R. R., Jr.; Bencosme, C. S.; Collman, J. P.; Anson, F. C. *J. Am. Chem. Soc.* **1983**, *105*, 2710−2718.
(21) Mest, Y. L.; Inisan, C.; Laouénan, A.; L'Her, M.; Talarmin, J.; Khalifa, M. L.; Saillard, J.-Y. *J. Am. Chem. Soc.* **1997**, *119*, 6095−6106.

JA0486216